

One-dimensional coherent four-wave mixing as a way to image the spatial distribution of atoms in a laser-produced plasma

D. A. Akimov, A. B. Fedotov, N. I. Koroteev,* A. N. Naumov, D. A. Sidorov-Biryukov, and A. M. Zheltikov

International Laser Center, Faculty of Physics, Moscow State University, Moscow, 119899 Russia

R. B. Miles

Department of Mechanical and Aerospace Engineering, Princeton University, Princeton, New Jersey 08544-5263

Received December 3, 1998

An experimental technique based on coherent one-dimensional hyper-Raman-resonant four-wave mixing in broad cylindrically focused light beams has been developed for line-by-line imaging of spatial distribution of excited atoms in a low-temperature plasma of optical breakdown. The technique was applied to map excited lead atoms in a low-temperature laser-produced plasma. © 1999 Optical Society of America

OCIS codes: 190.4380, 190.1900, 190.4180.

Until recently, laser-produced plasma has not been widely studied by use of coherent four-wave-mixing (FWM) spectroscopy,¹ although it has been known for quite a long time² that the cubic susceptibility of excited atoms and ions in a laser-produced plasma can be high enough to allow the generation of reliably detectable signals. The main difficulties encountered in FWM studies of laser-produced plasmas stem from intense plasma emission, a high nonresonant coherent background, and strong absorption and considerable phase-mismatch effects at certain stages of plasma expansion.³ The accuracy of nonlinear optical measurements in laser-produced plasmas is usually lowered by inevitable fluctuations of plasma parameters from pulse to pulse and by the complexity of FWM spectra. Luckily, coherent four-photon spectroscopy provides a rich variety of tools for solving the problems listed above. In particular, the level of incoherent background can be decreased by means of time gating and spatial filtering of the FWM signal, and the polarization FWM technique makes it possible to suppress the coherent background⁴ and to resolve closely spaced and overlapping lines related to different plasma species,⁵ eventually improving the sensitivity of FWM spectroscopy.

Fluctuations of plasma parameters is the main problem inherent in the diagnostics of laser-produced plasmas. Since each laser pulse, in fact, creates a new plasma, any averaging procedure gives rise to experimental errors and lowers the usefulness of laser diagnostics, especially when fast processes in spatially inhomogeneous plasmas have to be investigated.⁶ A radical solution to this problem is the application of folded FWM schemes in broad beams, providing information on spatial distributions of plasma parameters line by line or even slice by slice. The idea of using broad-beam coherent FWM to image the whole field of parameters of a gas medium rather than to get information from a single point is not new. Regnier and Taran⁷ discussed the possibility of implementing photographic detection of the anti-Stokes signal with a plane-wave geometry of light beams in coherent anti-Stokes Raman scattering^{4,7,8} (CARS) in 1973. Murphy *et al.*⁹ applied one-dimensional (1-D) vibrational CARS

with large-angle phase matching to the investigation of a CH₄ jet. Single-pulse spatially and spectrally resolved broadband rotational multipoint CARS along a line in a gas flow with the use of a large-angle folded geometry was implemented by Snow *et al.*¹⁰ Several convenient and elegant schemes have been developed for two-dimensional (2-D) imaging of temperature¹¹ and mapping of spatial distributions of species¹² in gas media with degenerate four-wave mixing (DFWM).¹³ A comprehensive analysis of many methodological problems of DFWM imaging, including diffraction effects, spatial resolution, and image referencing, has been provided by Ewart *et al.*¹⁴ FWM imaging along a line by use of vibrational CARS was performed by Jonuscheit *et al.*¹⁵

In this Letter we propose an experimental technique for imaging the relative populations of excited states of atoms in a decaying low-temperature plasma of optical breakdown induced on the surface of a metal target. This technique is based on three-color coherent FWM with hyper-Raman resonances,³⁻⁶ implying that a pair of cylindrically focused coplanar broad light beams forming a small angle irradiate a thin plasma layer in a plane parallel to the plane of the target. The third cylindrically focused light beam irradiates the laser-produced spark from above. The FWM signal is generated in the direction of phase matching. Imaging the interaction region onto a CCD array in FWM light, we can generate 2-D maps of the spatial distribution of resonant atoms in a plasma line by line.

The experimental setup consisted of a laser system for FWM plasma probing, a laser that produced optical breakdown, a timing unit, and the detection system. The probing laser system (described in detail in Ref. 3) was based on a Q-switched Nd:YAG master oscillator that generated 15-ns laser pulses at 1.064 μm . Amplified fundamental radiation was converted into the second harmonic with a cesium dehydroarsenate (CDA) crystal. Second-harmonic radiation was used to pump a dye laser that generated frequency-tunable radiation within the range 0.560–0.600 μm , with a bandwidth of $\sim 0.5 \text{ cm}^{-1}$. Since experimental errors were mainly associated with fluctuations of plasma parameters from pulse to pulse, beam referencing, i.e.,

compensating for intensity fluctuations along the profile of the dye-laser beam, did not produce a noticeable improvement in the accuracy of measurements and therefore was not used in experiments involving averaging over several laser pulses. The polarization of fundamental radiation was fixed, whereas the polarizations of the second harmonic and dye-laser radiation were varied by means of double Fresnel rhombs; this ensured the best contrast of FWM spectra.³ Such polarization control of FWM spectra allows one to improve the selectivity and sensitivity of FWM diagnostics, which may be especially useful for measuring the parameters of multicomponent plasmas, in which FWM spectra are complicated by multiple resonances. In this case, FWM can provide important information concerning spatial distributions of plasma parameters in addition to the accurate data that can be obtained for dominant atomic species by means of laser-induced plasma spectroscopy.¹⁶

The system for plasma excitation employed a Q-switched Nd:YAG master oscillator that generated 15-ns 200-mJ laser pulses. A laser beam produced by this system was focused on the surface of a metal target with a 10-cm focal-length cylindrical lens. Rotating this lens, we were able to vary the orientation of a laser-produced spark with respect to the incident beams. The plasma was irradiated by three-color pumping beams with a variable delay time τ with respect to plasma excitation.

The implemented experimental technique for plasma imaging employs three-color coherent FWM with hyper-Raman resonances, in which the frequency of the FWM signal $\omega_{\text{FWM}} = \omega_1 + \omega_2 - \omega_3$ (where ω_3 is the frequency of fundamental radiation of a Nd:YAG laser, ω_1 is the frequency of the second harmonic of a Nd:YAG laser, and ω_2 is the frequency of a tunable dye laser) is resonant to some atomic (or ionic) transition in a laser-produced plasma. In our experiments we chose the frequency of the dye laser to ensure a resonance between the frequency ω_{FWM} and the frequency of the $7s\ ^3P_0 - 6p^2\ ^3P_1$ transition in Pb atoms [Fig. 1(a)] in a laser-produced plasma created on the surface of a lead target. Under these conditions, we observed a resonant enhancement of the FWM signal at 368.45 nm owing to a hyper-Raman resonance. In an expanding plasma the populations N_1 and N_2 of resonant levels 1 and 2 [Fig. 1(a)] change with time. Numerical simulations performed for this transition demonstrate that, at least for τ of 400 ns between plasma excitation and probing, the population of level 2 is much less than the population of level 1, and the population difference $N = N_1 - N_2$ is close to the population of level 1. At early stages of plasma expansion, i.e., for small τ , the dependence of P_{FWM} on the concentration of resonant species can deviate from N^2 owing to phase-mismatch and absorption effects.³ However, for sufficiently large τ ($\tau > 2.0\ \mu\text{s}$ for the transition of Pb atoms in our experimental conditions), P_{FWM} can be approximated with a quadratic function of N , and the maps of the FWM signal provide undistorted information on the spatial distribution of Pb atoms in a plasma. To avoid the influence of one-photon absorption and

phase mismatch, we performed FWM plasma imaging for $\tau = 3.0\ \mu\text{s}$.

The second-harmonic (pump wave ω_1) and the dye-laser (pump wave ω_2) beams, focused with a 10-cm focal-length cylindrical lens, formed coplanar broad light sheets with wave vectors \mathbf{k}_1 and \mathbf{k}_2 , forming a small angle θ [Fig. 1(b)], and sizes of $4\ \text{mm} \times 20\ \mu\text{m}$ in the beam-waist area. These beams irradiated a thin plasma layer in a plane parallel to the plane of the target. A cylindrically focused beam with frequency ω_3 and wave vector \mathbf{k}_3 , which made an angle α with the plane of the \mathbf{k}_1 and \mathbf{k}_2 vectors, irradiated the laser-produced spark from above [Fig. 1(c)]. The FWM signal is generated in the direction \mathbf{k}_{FWM} determined by phase-matching conditions, forming an angle β with the plane of the target [Figs. 1(b) and 1(c)]. Imaging the one-dimensional FWM signal onto a CCD array, we were able to map the spatial distribution of resonant particles in the plasma line by line. To reduce the level of plasma-emission background we placed the CCD array at a distance of $\sim 80\ \text{cm}$ from the spark and used a slit for spatial filtering.

The 2-D map shown in Fig. 2 was obtained with $\theta = 0$ and $\alpha \approx 3^\circ$ in the transverse [see Fig. 1(c)] scheme of plasma imaging. The 1-D FWM signal

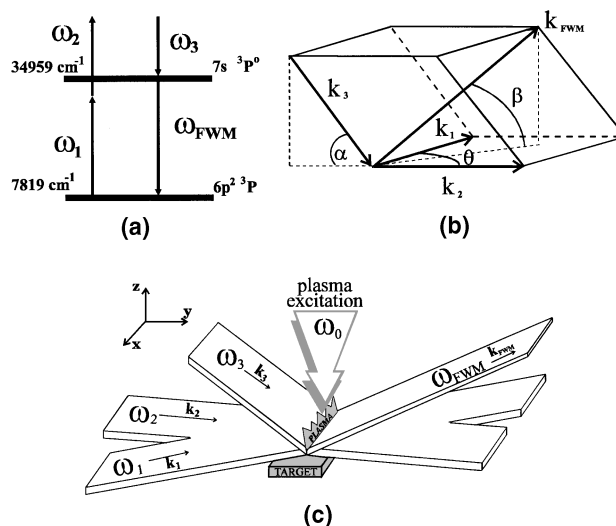


Fig. 1. One-dimensional imaging of atoms in a laser-produced plasma by means of coherent hyper-Raman resonant FWM in broad beams: (a) diagram of a four-photon process with a hyper-Raman resonance involving excited states of a lead atom, (b) diagram of wave vectors, and (c) diagram of light beams.

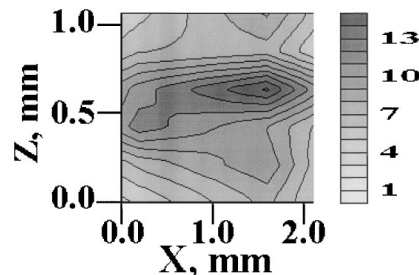


Fig. 2. Line-by-line plasma imaging with 1-D FWM in the transverse direction: 2-D map of the FWM signal power with a resonance that is due to Pb atomic transitions.

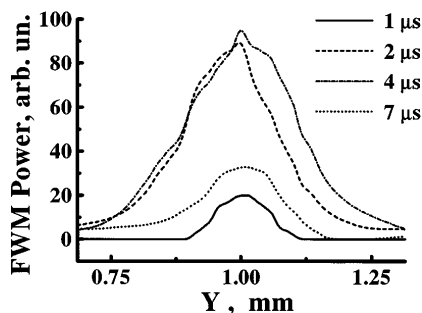


Fig. 3. 1-D FWM signals imaging a plasma area located at a distance of 0.5 mm from the target surface at the center of the plasma spark along the x axis at delay times $\tau = 1, 2, 4, 7 \mu\text{s}$.

in our scheme can be employed to image the spatial distribution of Pb atoms along the line corresponding to the intersection of the light beams with wave vectors \mathbf{k}_1 , \mathbf{k}_2 , and \mathbf{k}_3 [see Fig. 1(c)]. However, to compose a 2-D image of some plasma area we have to scan the plasma with respect to laser beams, which means that averaging should be performed to smooth out fluctuations in plasma parameters from pulse to pulse. Each line in the 2-D map shown in Fig. 2 represents the result of averaging over 100 laser pulses. Since the FWM signal intensity is a nonlinear (quadratic) function of the density of resonant species, such an averaging procedure gives rise to systematic deviations of FWM images from real spatial distributions of resonant species. In our experiments, such a deviation for resonant Pb atoms was estimated as approximately 2%. Averaged density profiles of Pb atoms measured by means of 1-D FWM correlated fairly well with the averaged results of point-by-point FWM measurements.^{3,6} Figure 3 shows how the 1-D FWM signal from a plasma changes with delay time τ . While the 1-D FWM signal recorded at $\tau \approx 1 \mu\text{s}$ is subject to the influence of phase mismatch and absorption, 1-D signals measured at $\tau = 2, 4, 7 \mu\text{s}$ provide the information on time evolution of the spatial distribution of excited Pb atoms in the plasma.

The spatial resolution in the three-color folded FWM imaging scheme described above is determined by the geometry of FWM interaction and can be adequately specified in terms of geometric sizes of the interaction area. For our scheme these sizes were estimated as 14 and 680 μm along small and large dimensions of sheetlike incident beams, respectively. Therefore, each line in 1-D FWM in our experiments corresponds to a signal collected from a 680 $\mu\text{m} \times 14 \mu\text{m}$ plasma element, providing an opportunity to resolve plasma volumes with such dimensions (the spatial resolution along a CCD array in the direction perpendicular to the wave vector \mathbf{k}_{FWM} is determined by the resolution of the imaging system). The sensitivity of line-by-line FWM imaging of Pb atoms in our scheme for $\tau \approx 3.0 \mu\text{s}$ is estimated as 10^{13} cm^{-3} . Since the main source of noise in such experiments is associated with plasma emission, the sensitivity of FWM imaging technique can be further improved with a careful spatial and temporal filtering of the FWM signal.

The experimental results presented here demonstrate that 1-D coherent FWM with hyper-Raman resonances allows line-by-line imaging of the spatial distribution of excited atoms in a plasma of optical breakdown. The basic advantage of the proposed approach is that it generates plasma maps line by line, which reduces the number of measurements and improves the reliability of plasma analysis compared with that of point-by-point imaging. Such a procedure holds much promise for the investigation of spatially inhomogeneous fast processes in a multicomponent laser-produced plasma.

This research was supported in part by Award RP1-255 of the U.S. Civilian Research and Development Foundation for the Independent States of the Former Soviet Union (CRDF). A. M. Zheltikov's e-mail address is zhelt@ilc.phys.msu.su.

*N. I. Koroteev is deceased.

References

1. N. Bloembergen, *Nonlinear Optics* (Benjamin, New York, 1965); Y. R. Shen, *The Principles of Nonlinear Optics* (Wiley, New York, 1984); A. C. Eckbreth, *Laser Diagnostics for Combustion Temperature and Species* (Abacus, Cambridge, 1988).
2. S. M. Gladkov, A. M. Zheltikov, N. I. Koroteev, I. S. Koleva, and A. B. Fedotov, *Sov. Tech. Phys. Lett.* **15**, 505 (1989).
3. A. B. Fedotov, N. I. Koroteev, A. N. Naumov, D. A. Sidorov-Biryukov, and A. M. Zheltikov, *J. Nonlinear Opt. Phys. Mater.* **6**, 387 (1997).
4. S. A. Akhmanov and N. I. Koroteev, *Methods of Nonlinear Optics in Spectroscopy of Light Scattering* (Nauka, Moscow, 1981).
5. N. I. Koroteev, A. N. Naumov, D. A. Sidorov-Biryukov, and A. M. Zheltikov, *Laser Phys.* **7**, 45 (1997).
6. D. A. Akimov, A. B. Fedotov, N. I. Koroteev, A. N. Naumov, D. A. Sidorov-Biryukov, and A. M. Zheltikov, *Opt. Commun.* **140**, 259 (1997).
7. P. R. Regnier and J. P.-E. Taran, *Appl. Phys. Lett.* **23**, 240 (1973).
8. S. Druet and J.-P. Taran, *Prog. Quantum Electron.* **7**, 1 (1981).
9. D. V. Murphy, M. B. Long, R. K. Chang, and A. C. Eckbreth, *Opt. Lett.* **4**, 167 (1979).
10. J. B. Snow, J. Zheng, and R. K. Chang, *Opt. Lett.* **8**, 599 (1983).
11. P. Ewart and M. Kaczmarek, *Appl. Opt.* **30**, 3996 (1991); K. Nyholm, R. Fritzon, and M. Alden, *Appl. Phys. B* **59**, 37 (1994).
12. P. Ewart, P. Snowdon, and I. Magnusson, *Opt. Lett.* **14**, 563 (1989); D. J. Rakestraw, R. L. Farrow, and T. Dreier, *Opt. Lett.* **15**, 709 (1990).
13. R. L. Abrams and R. C. Lind, *Opt. Lett.* **2**, 94 (1978); R. A. Fisher, *Optical Phase Conjugation* (Academic, London, 1983); J. Pender and L. Hesselink, *Opt. Lett.* **10**, 264 (1985).
14. P. Ewart, P. G. R. Smith, and R. B. Williams, *Appl. Opt.* **36**, 5959 (1997).
15. J. Jonuscheit, A. Thumann, M. Schenk, T. Seeger, and A. Leipertz, *Opt. Lett.* **21**, 1532 (1996); *Appl. Opt.* **36**, 3253 (1997).
16. R. Wisbrun, I. Schechter, R. Niessner, and H. Schroeder, *Proc. SPIE* **1716**, 2 (1993).